Pressure Probe Measurements of Turbulent Flow in a Spray Drier With a Rotary Atomiser

G. D. Sizgek,[1] E. Sizgek[1] and J. D. Hooper[2]

[1]Australian Nuclear Science and Technology Organisation
PMB 1, Menai, NSW, 2234

[2]Turbulent Flow Instrumentation Pty Ltd
1 Blackbutt Place, Engadine, NSW Australia 2233

ABSTRACT

This study includes experimental and numerical characterisation of the gas flow behaviour at the inlet and in the region near rotary atomiser in a pilot scale (1.2 m diameter) co-current spray drier. Numerical calculations were based on the commercial computational fluid dynamics code CFX4 (AEA Technology, 1995).

Measurements of the turbulent flow behaviour were conducted using an improved frequency response, four hole pressure probe (known as the Cobra probe) to test the numerical predictions. The probe resolves simultaneously all components of the mean velocity and Reynolds stresses at a point in the flow. Measurements were carried out both at the presence of disc rotation (20000 rpm.) and when there is no rotation. Experiments and predictions were in satisfactory agreement in both conditions. Results revealed that disc rotation (compared to no rotation) did not have much effect on the flow field in the inlet region. It was apparent from very high levels of turbulence intensity and the high magnitude of the tangential velocity component in the region around the rotating disc that the rotating disc was the major source of swirl in the drier cabinet.

1. INTRODUCTION

Spray drying is one of the most important continuous drying techniques to produce powder from fluid feeds (solutions, emulsions, slurries and pumpable pastes). This unit operation is common to many industries with the products ranging from minerals and heavy chemicals to pharmaceuticals and processed foods. Although its wide range usage, spray drier design is still difficult due to the complexity of the atomisation and spray-gas interactions. Accurate simulation of gas flow patterns without spray is an important first step before simulating gas-spray interaction in the drier. Recently highly sophisticated commercial Computational Fluid Dynamics software packages have made it possible to predict air flow patterns and to some extent gas-spray mixing in the drier chamber. A detailed characterisation of the flow pattern in the region around the rotating disk and inlet section of the spray drier will help to better understand mechanisms responsible for the evaporation rates of the atomised particles.

The probable air flow pattern produced by rotating disk inside a spray drier was discussed by Masters (1985). Later, measurements of velocity components by Keey et al. (1991) using four-hole pitot tube and visualisation by Langrish et al. (1992) of the air flow patterns inside pilot scale driers with rotating atomisers were carried out. They have shown the interactions between entering air and air pumped by the rotary atomiser. In the present paper, a high frequency four-hole pressure probe was used to measure quantitatively all components of velocity and Reynolds stresses at the inlet and in the vicinity of the rotating disk in the spray drier.

This study is the first part of the project to aid operation and scale-up for spray drying of sol-gel based colloid systems to produce Synroc ceramic microspheres. The objective of this work was to test the CFD model predictions against the measurements of air flow inside the spray drier fitted with a rotary atomiser.

2. EXPERIMENTAL

Spray drier

The spray drier chamber used in this work (Figure 1) is a pilot scale spray drier (Niro, model P6.3). It consists of a cylindrical section, 1.2 m in diameter and 0.78 m tall, with a conical bottom 0.78 m long. Air supplied through a horizontal tube and the air disperser flows through the annular inlet opening around the atomiser into the drying chamber. The width of the annulus is 20 mm. A rotary atomiser drive assembly (model FU-11) is centrally located in the roof of the drying chamber. A variable speed motor enables the 120 mm diameter rotary disk to spin at a speeds between 0 and 25000 rev/min.

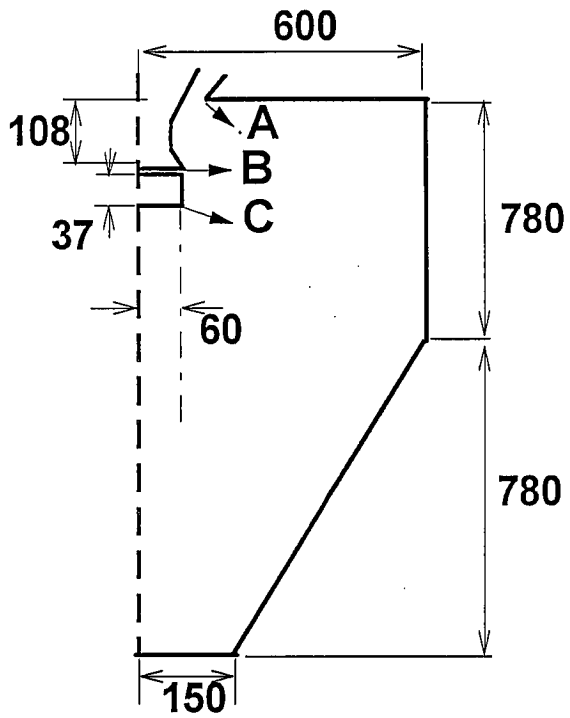

Figure 1 Spray Drier (dimensions in millimetres)

During measurements a rotation speed of 20000 rev/min was used and no spray was present. Also measurements were repeated when the disc was stationary. Ambient conditions were used during the measurements and the air flow was kept at 385 m^3/h. The door of drying chamber was replaced with a two-piece steel cover to provide good access for high frequency cobra probe system.

Pressure probe

An improved frequency response, four-hole pressure probe (known as the Cobra probe) (Hooper and Musgrove, 1995; Musgrove and Hooper, 1995) has been used to measure simultaneously all components of velocity and Reynolds stresses across the annular inlet and around the atomiser disc. The probe used for measurements had a tap hole diameter 0.5 mm, a head width of 2.6 mm and 200 mm of pressure tubing separating the pressure transducers from the tip. The Cobra probe was mounted on a computer driven radial traverse system with 360 degrees of rotation in the yaw plane of the probe. The traverse was placed on a frame outside the drying chamber to ensure minimum flow interference. The probe was mounted on a 19 mm diameter rod which had a total reach of 1.3 m. An automatic search routine, using sixteen equal increments in yaw, was used to locate the yaw angle at which the probe centre pressure was a maximum.

3. NUMERICAL MODEL

The numerical simulations of air flow in the spray drier chamber have been carried out using the computational dynamics code CFX4 (version 4.1.b). The code uses standard finite difference techniques to generate approximations to the conservation equations on a body fitted three dimensional grid.

The simulations presented here are cylindrical, axisymmetrical and two dimensional. Except in the case of swirling flows (the swirl component of velocity destroys the symmetry), the model is treated as three dimensional with the number of cells in the theta direction equal to one. The standard k-ε and also the Differential Reynolds stress turbulence models were employed to model the effects of the turbulence on the flow.

Introducing the atomiser disc rotation to the model increased the computational effort, which required considerably finer grid and more iterations for conversion, compared to the no disc rotation case. Three grid sizes were used in the simulation to assess the grid independence of the numerical solution. The

grid size of 9600 cells (Figure 2) was used in the calculations presented here.

Inlet values of the velocity components and all components of Reynolds stresses were measured at the annular inlet where the flow enters into the drier chamber. The inlet velocity was the same when the disc was rotating and stationary.

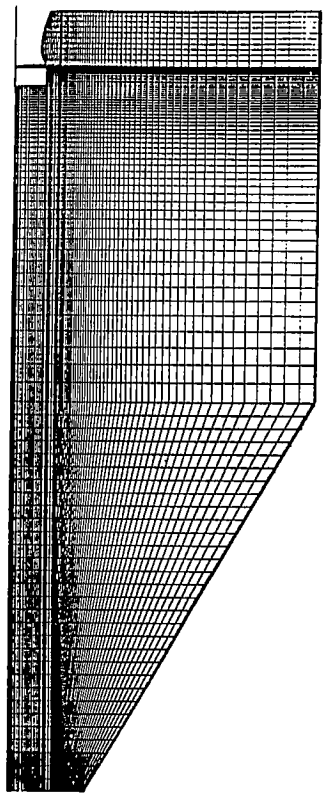

Figure 2 Computational grid.

These inlet values were used in the numerical simulation. The average measured values of these quantities across the inlet are given in Table 1. The turbulent kinetic energy at the inlet is given by $k = 0.5\,(u'^2 + v'^2 + w'^2)$.

Table 1 Measured quantities at the inlet.

velocity components	Fluctuating components of velocity	Reynolds shear stresses
u = 10.6 m/s	u' =1.1 m/s	uv=0.3 m^2/s^2
v = 2.6 m/s	v' =0.8 m/s	uw=0.1 m^2/s^2
w = 1.5 m/s	w' =0.8 m/s	vw=0.1 m^2/s^2

4. RESULTS AND DISCUSSION

Results from the experimental pressure probe measurements and numerical calculations are presented and discussed in three sections. The first section is the inlet region between the point A and B (Figure 1). The second section is near the rotating disc between point B and C (Figure 1) and the third section is below the rotating disc (below point C).

During measurements the flow at each radial position was scanned at 2.5 mm increments upto the region where the mean flow was low, with the difference between the local dynamic and static pressures beyond the resolution of the pressure transducers. The Cobra probe was found to be insensitive below a mean velocity of 4 m/s. The probe measurements were reliable in all flow regions except within the 10 mm of the disc surface when the disc was rotating.

Numerical predictions show that when the disc is stationary the calculations based on the standard k-ε turbulence model resemble the predictions based on the Differential Reynolds stress model. But for the case of disc rotation, especially in the vicinity of the disc, the Differential Reynolds stress model gives closer predictions to the measured values of the radial and tangential velocities than the standard k-ε turbulence model. Thus numerical predictions based on the Differential Reynolds stress model will be discussed here.

In all graphs the vertical surface of the disc is shown as the zero axis. The label 'r' of the abscissa represents the distance from the surface of the disk.

Inlet region

The inlet measurements (Table 1) reveal that the entering air has a very low swirl and the axial component of velocity dominates the main flow. The experimentally determined axial, radial and tangential velocity profiles below the inlet for (a) the rotating disc at 20000 rpm and (b) no rotation are shown in Figure 3, for the five axial positions as function of radial distance. The measurements at each radial position were started 2 mm from the atomiser cone. Flow at the inlet region shows similar

characteristics when the disc is rotating and stationary. This suggests that rotation of the disc has not much influence in the inlet region, except the swirl component of the velocity changes direction in the case of disc rotation. In both cases, the air jet entering through the annular inlet, at the drier ceiling next to atomiser cone, has an outer boundary at a distance about 75 mm from the drier axis. These findings are consistent with the numerical predictions (Figure 4 (a) and (b)) for both cases.

The agreement between the measured and predicted axial velocity profiles is quite satisfactory especially away from the atomiser surface. However, the calculated radial and tangential velocities in Figure 4 (a) and (b) are smaller than those of measured values and the agreements are rather qualitative.

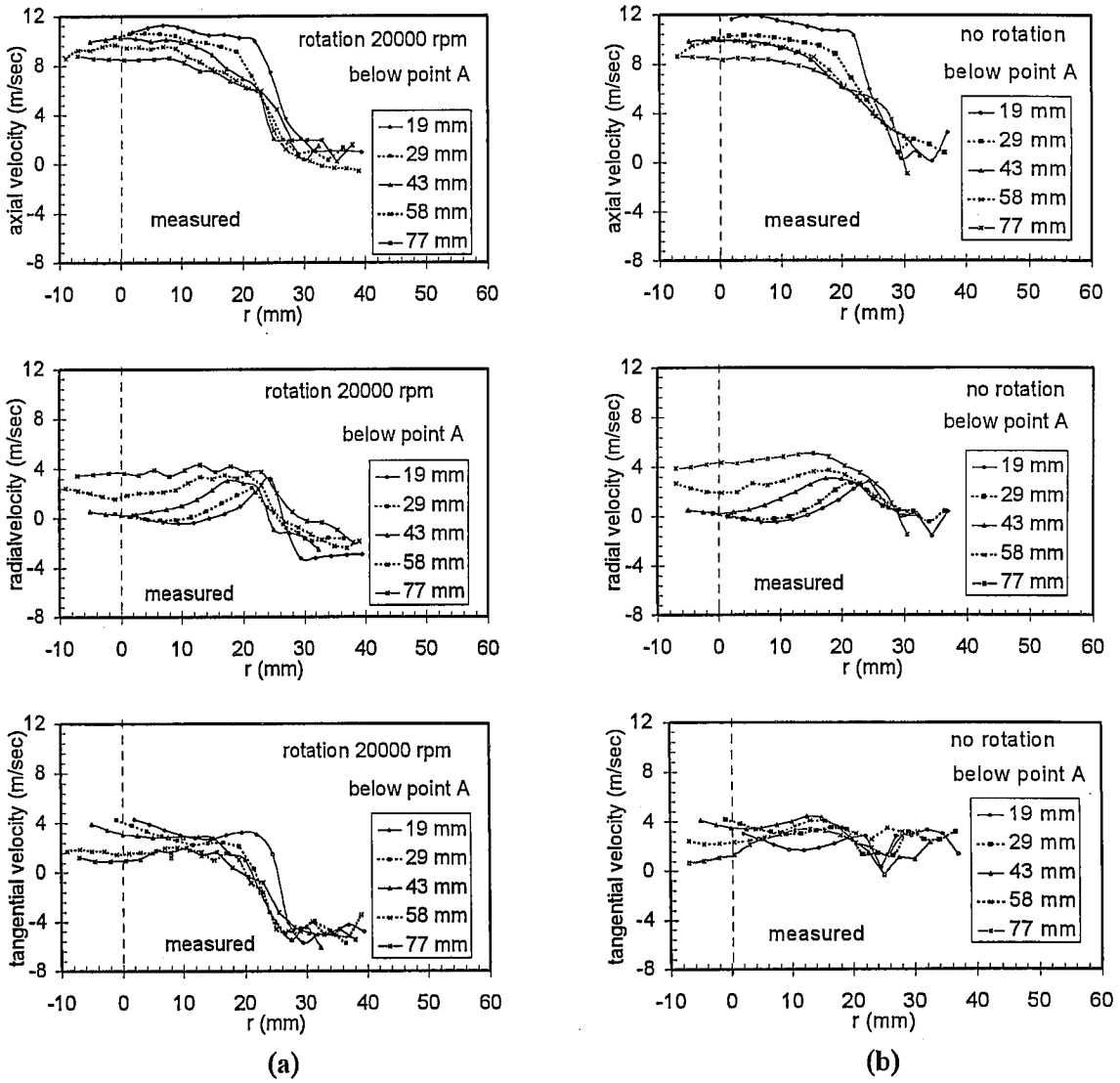

Figure 3 Radial distribution of measured velocity components at the inlet region above the atomiser disc (Conditions as given in text). **(a)** rotation 20000 rpm; **(b)** no rotation of disc.

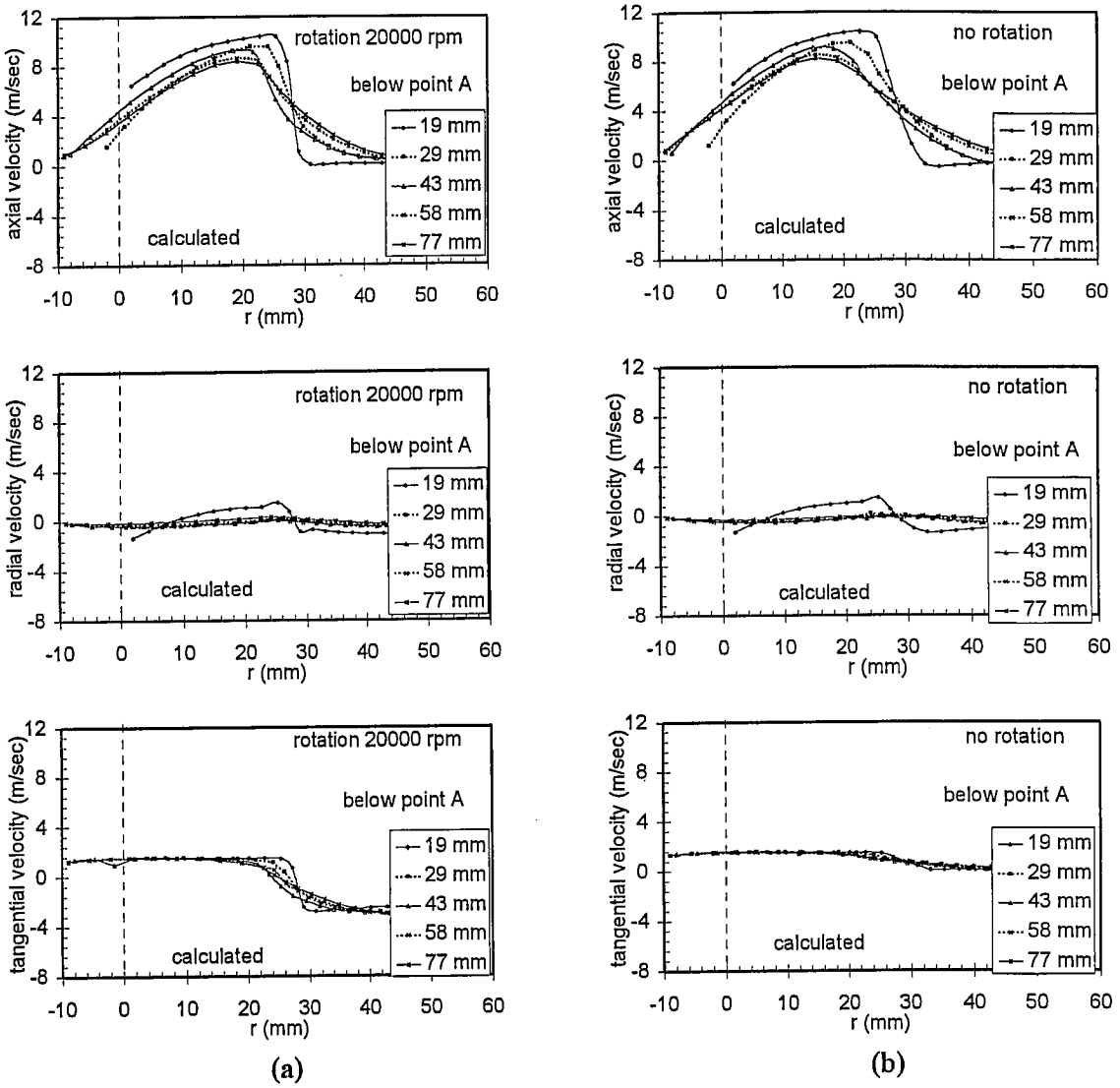

Figure 4 Radial distribution of predicted (Differential Reynolds Stress model) velocity components at the inlet region above the atomiser disc. (Conditions as given in text). **(a)** rotation 20000 rpm; **(b)** no rotation of disc.

Disc region

The radial distribution of measured velocity components conducted at five heights along the rotating disc surface is given in Figure 5 (a).

Point B (Figure 1) is in the middle of the gap between the stationary atomiser cone and the rotating disc. Measurements at the point B show that still the axial component of velocity is dominant one and the radial and tangential velocities are almost negligible. In the rotating disc region the axial velocity component of downward jet suddenly decays and radial, especially tangential components of velocity govern the main flow (Figure 5 (a)). The similar trend is observed with the calculated results in Figure 5(b). The difference is that the predicted tangential velocities compared to the measured ones diminish sharply within 35 mm of the disc surface. And also calculated radial velocities are lower than the measures ones.

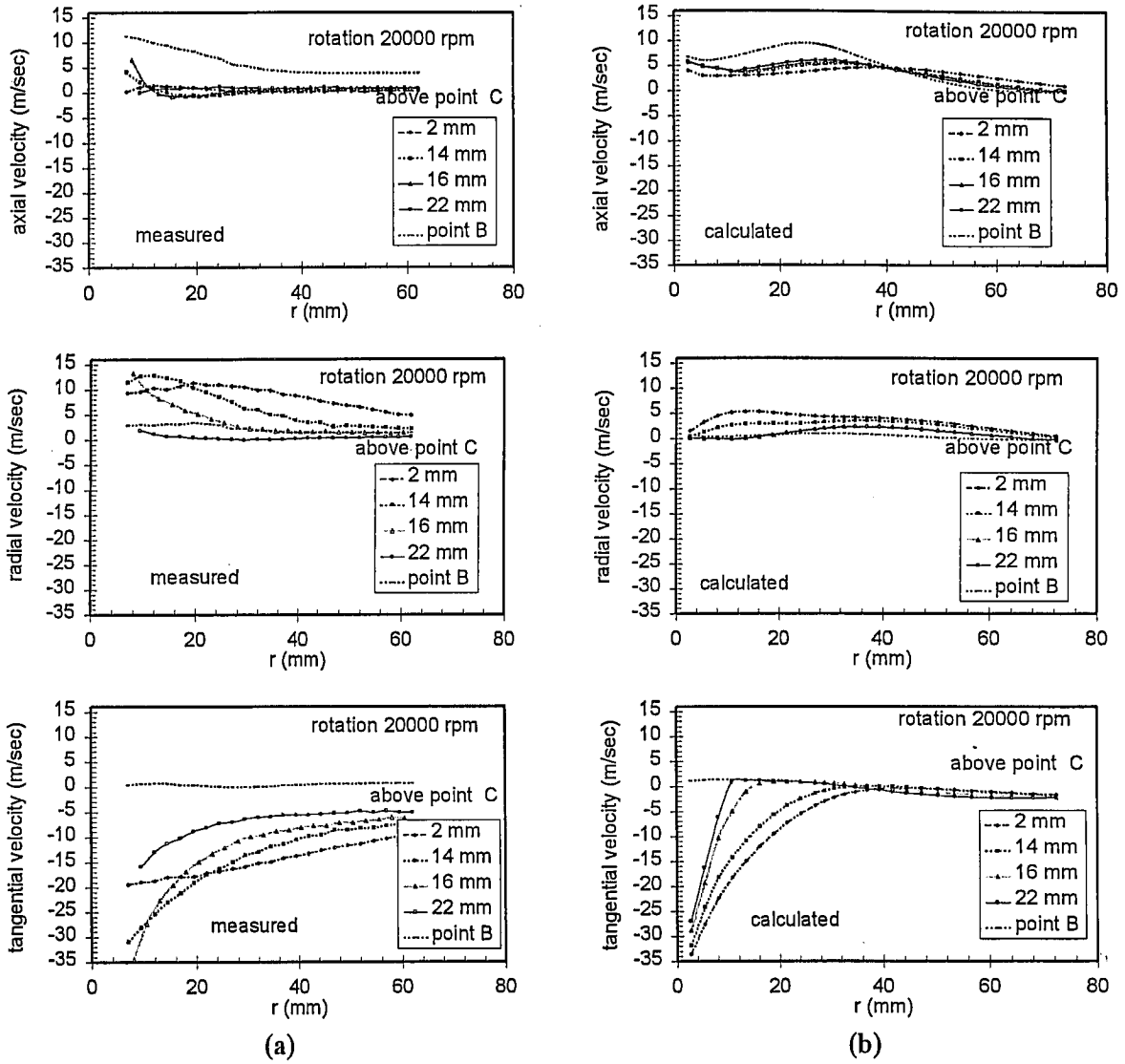

Figure 5 Radial distribution of velocity components around the rotating disc. (Conditions as given in text). (a) measured; (b) predicted (Differential Reynolds Stress model).

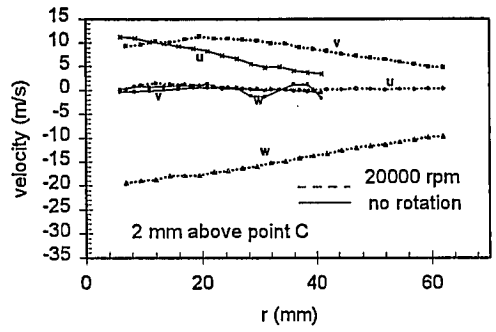

Figure 6 Comparison of measured velocity components for rotation and no rotation cases in the vicinity of the disc (2 mm above point C)

Comparison of velocity profiles measured close to the lower corner of the disc surface for rotation and no rotation cases is given in Figure 6. It is clear that with the rotation the mean flow diverges from the solid surface of the rotating disc.

Plots of measured and calculated root mean square fluctuating velocities (RMS) for the same position are shown in Figure 7. These RMS velocities are directly related to the normal components of Reynolds stresses.

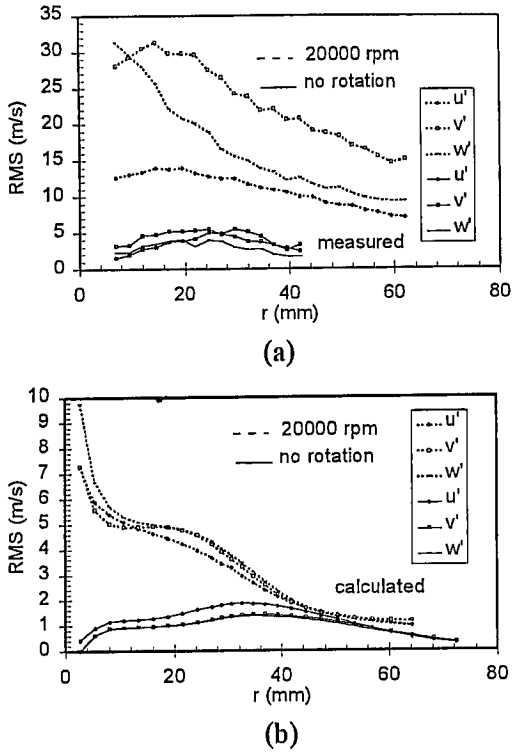

Figure 7 (a) Measured and (b) Predicted axial (u'), radial (v') and tangential (w') fluctuating velocities at 2 mm above point C.

The highly sheared flow adjacent to the spinning disc is shown by the large induced radial and tangential mean velocities (Figure 5 (a)), and the large magnitude of the radial and tangential turbulence intensities (Figure 7 (a)) in this area. The measured mean tangential velocity profile here shows generally a lower radial gradient than the calculated profile. However, the experimental turbulence intensities are approximately three times larger than the calculated values. This region of the drier is of particular interest, as it is where droplet break-up occurs.

Figure 8 shows the measured and calculated Reynolds shear stresses which indicate correlations between the fluctuating velocities. For the no rotation case there is almost no correlation between the fluctuating velocities. For the disc rotation case, high values of Reynolds stresses near the disc imply strong correlation between the fluctuating velocities. Numerical predictions show better agreement with the measured values near the disc than farther away from the disc.

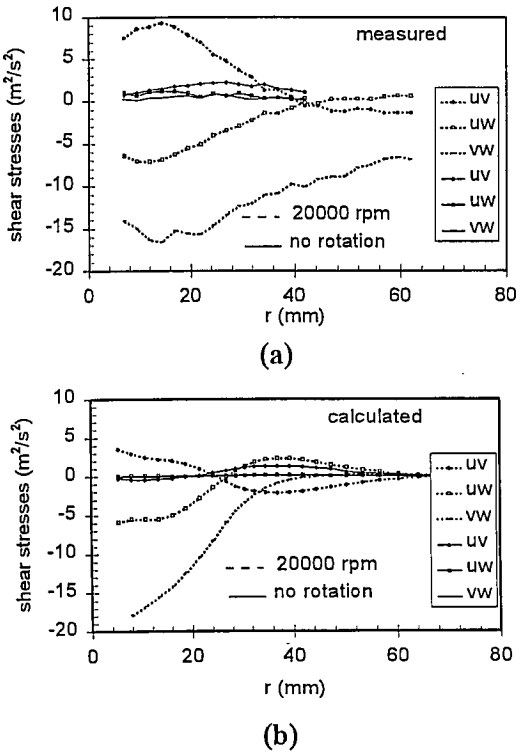

Figure 8 Measured and predicted Reynolds shear stresses at 2 mm above point C.

Below disc region

The velocity measurements below the atomiser disc are given in Figure 9 for the disc rotation and no rotation cases. For the disc rotation case, below the disc, high values of tangential and radial velocities indicate the effect of disc rotation. Both velocities show a maximum at a distance 30 mm away from the spray drier axis (-60 shows the drier axis). For the no rotation case (Figure 9(b)), high axial velocity component indicates that downward jet from the inlet region continues. Agreement between the calculated (Figure 10) and measured velocities is rather qualitative although model predictions for no rotation case (Figure 10(b)) are better than the disc rotation case for this region.

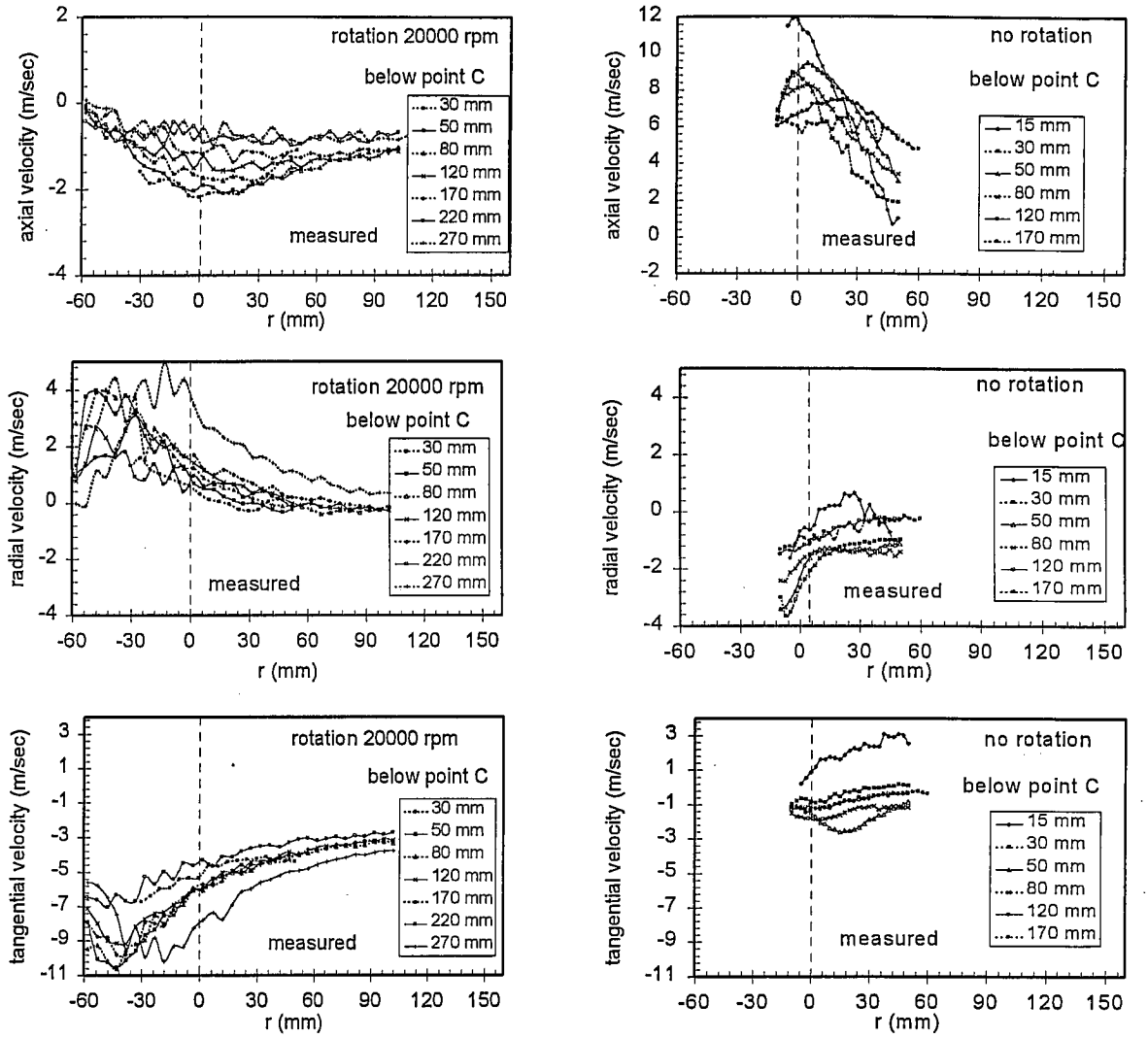

Figure 9 Radial distribution of measured velocity components in the region below the atomiser disc. (Conditions as given in text). **(a)** rotation 20000 rpm; **(b)** no rotation of disc.

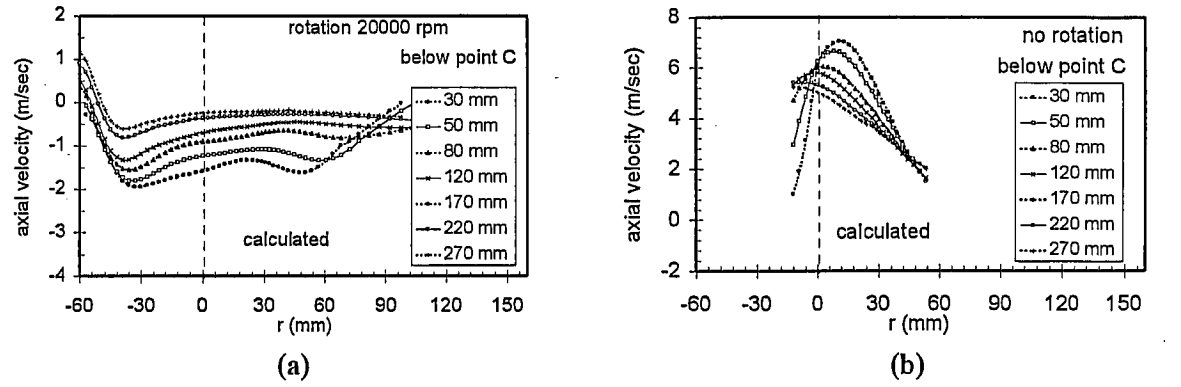

Figure 10 Continued on the next page

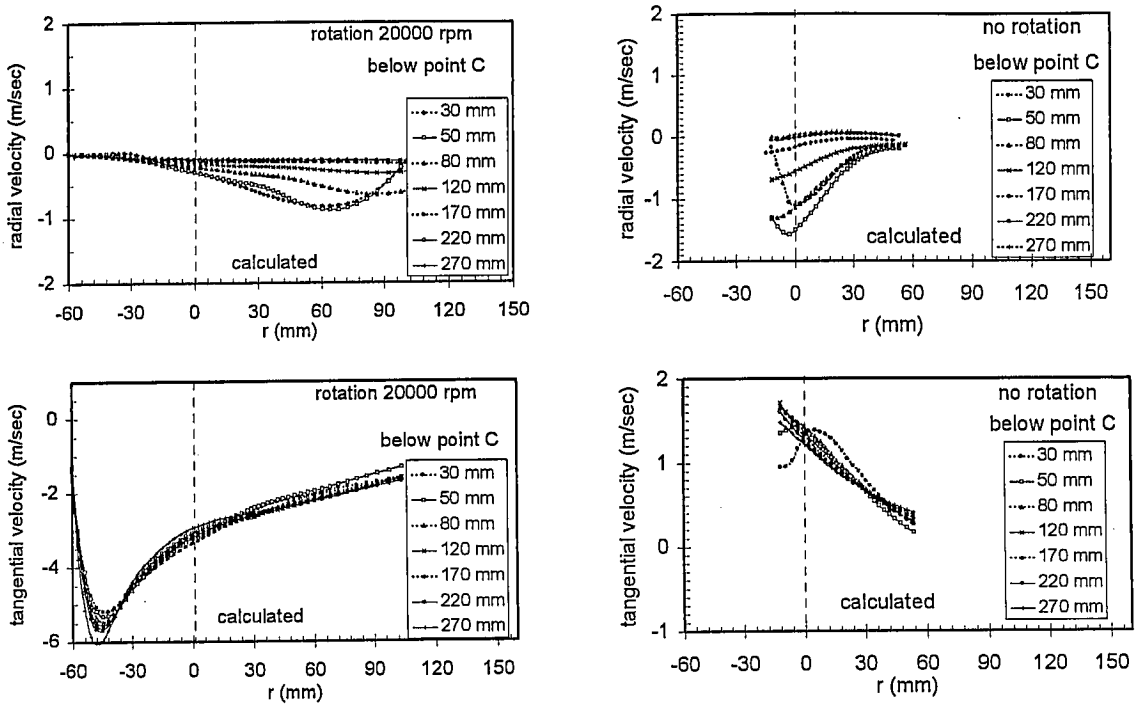

Figure 10 Radial distribution of predicted (Differential Reynolds Stress model) velocity components (axial, radial and tangential) in the region below the atomiser disc. (Conditions as given in text). **(a)** rotation 20000 rpm; **(b)** no rotation of disc.

5. CONCLUSIONS

The four hole Cobra probe has been shown to be able to measure the turbulent distributions in the vicinity of the rotating atomiser for the conditions studied here. The measurements and predictions appear to agree satisfactorily in the inlet region where the air enters to the drier chamber. The disc rotation does not seem to have any effect in this region. Further down from the inlet, below the atomiser disc, the agreement between the numerical model and predictions is not so well, but it is still reasonable. For the spinning disc case the Differential Reynolds stress model gives better results than k-ε turbulence model. The model predicts correctly a diverging flow from the spinning disc surface, though the experimental turbulence intensities are somewhat higher than the calculated ones. Consistent with the measurements and predictions, disc rotation has pronounced effects on the turbulent structure around the disc. The high magnitude of tangential velocity component and high levels of turbulence intensity suggest that the rotating disc is the major source of swirl in the drier used in this study.

REFERENCES

AEA Technology, 1995, CFX 4.1 Flow solver, User Guide, Harwell Lab., Oxfordshire, UK.

Hooper, J.D. and Musgrove, A.R. del., 1995, "Pressure Probe Measurements of Reynolds Stresses and Static Pressure Fluctuations in Developed Pipe Flow", 12th Australasian Fluid Mech. Conf. Sydney, Australia, pp. 565 - 568.

Keey, R.B., Enevoldsen, S.S and Werner, C., "Air Pumping Behaviour of Rotary Atomisers". A.S. Mujumdar (ed), Drying'91, pp. 314-324.

Langrish, T.A.G., Keey, R.B. and Hutchinson, C.A., 1992, "Flow Visualisation in a Spray Drier Fitted with a Vaned-Wheel Atomiser". Trans IChemE, Vol. 70 (A), pp. 385-394.

Masters, K., 1985, "Spray Drying Handbook", 4th edn, Leonard Hill, London.

Musgrove, A.R. del. and Hooper, J.D., 1995, "Pressure-Velocity Correlations in Swirling Pipe Flow", 12th Australasian Fluid Mech.Conf. Sydney, Australia, pp. 557 -560.